



OPEN

Dielectric Characterization of a Nonlinear Optical Material

P. Lunkenheimer¹, S. Krohns¹, F. Gemander^{2*}, W. W. Schmahl² & A. Loidl¹

SUBJECT AREAS:

FERROELECTRICS AND
MULTIFERROICSELECTRONIC PROPERTIES AND
MATERIALSReceived
26 March 2014Accepted
24 July 2014Published
11 August 2014Correspondence and
requests for materials
should be addressed to
P.L. (peter.
lunkenheimer@physik.
uni-augsburg.de)* Current address:
Centrum Baustoffe und
Materialprüfung,
Baumbachstraße 7,
Technical University
Munich, 81245
Munich, Germany.¹Experimental Physics V, Center for Electronic Correlations and Magnetism, University of Augsburg, 86135 Augsburg, Germany, ²Department of Earth and Environmental Sciences, Materials Research, LMU Munich, 80333 Munich, Germany.

Batisite was reported to be a nonlinear optical material showing second harmonic generation. Using dielectric spectroscopy and polarization measurements, we provide a thorough investigation of the dielectric and charge-transport properties of this material. Batisite shows the typical characteristics of a linear lossy dielectric. No evidence for ferro- or antiferroelectric polarization is found. As the second-harmonic generation observed in batisite points to a non-centrosymmetric structure, this material is piezoelectric, but most likely not ferroelectric. In addition, we found evidence for hopping charge transport of localized charge carriers and a relaxational process at low temperatures.

Batisite, $\text{Na}_2\text{Ba}(\text{TiO})_2\text{Si}_4\text{O}_{12}$, was reported to show second-harmonic generation (SHG), implying a nonlinear dielectric susceptibility at optical frequencies¹. As SHG (at least in its leading electric-dipole order) requires the absence of crystalline inversion symmetry, this finding points to a non-centrosymmetric structure of this material^{2,3}. Indeed such a structure (space group $\text{Ima}2$) was reported for batisite in ref. 4. However, it should be noted that in ref. 5 a crystal-structure refinement of batisite was found to be well consistent with a centric structure (Imam). Generally, non-centrosymmetric crystals are piezoelectric and piezoelectricity indeed was reported for batisite⁶. However, the lack of inversion symmetry can, in addition, also lead to ferro- or antiferroelectricity, whose possible occurrence in this material was never checked. These polar states show typical signatures in dielectric spectroscopy, e.g., a peak or jump in the temperature dependence of the dielectric constant ϵ' , and a hysteresis in the electric-field dependent polarization⁷. In the present work, we provide a thorough investigation of the temperature and frequency dependence of the dielectric properties and conductivity of batisite. In addition, polarization measurements are reported. We find no indications of ferro- or antiferroelectric order. Batisite is a lossy dielectric and shows the signature of hopping charge transport and a weak relaxational process.

Results

Figure 1 shows the temperature dependence of the dielectric constant ϵ' (a) and the conductivity σ' (b) of batisite as measured for various frequencies. At high frequencies, $\epsilon'(T)$ exhibits moderate temperature dependence only; e.g., for 3.53 MHz it increases by about a factor of three between 62 and 666 K [Fig. 1(a)]. In contrast, at low frequencies $\epsilon'(T)$ rises up to about 10^4 at high temperatures. Such high values of the dielectric constant, sometimes termed “colossal dielectric constants”, can be caused by many different physical mechanisms⁸, including ferroelectric ordering. In a typical ferroelectric, when approaching the phase transition at T_c from high temperatures, $\epsilon'(T)$ strongly increases and starts to decrease again below T_c ⁷. Thus, when considering the 1 Hz curve in Fig. 1(a), at first glance one may suspect a ferroelectric phase transition at a temperature beyond the investigated temperature range. However, the strong frequency dependence of ϵ' , observed already at very low frequencies, speaks against ferroelectric ordering of batisite.

The conductivity of batisite [Fig. 1(b)] exhibits a general trend to increase with increasing temperature as expected for a non-metallic material. Superimposed to this trend, maxima or shoulders appear in $\sigma'(v)$, which shift to higher temperatures with increasing measurement frequency. Taking into account the general relation $\epsilon'' \propto \sigma'/v$, comparable peaks also arise in the dielectric loss, $\epsilon''(T)$ (not shown). Such a behaviour is typical for relaxation processes, which can be caused, e.g., by the reorientation of dipolar degrees of freedom in response to the ac electric field^{9,10}. The loss peaks should be accompanied by a steplike decrease of $\epsilon'(T)$ at low temperatures, where the mobility of the dipolar entities becomes too slow to follow the alternating field. Indeed such steps are observed in Fig. 1(a), especially at $T < 300$ K where they are not concealed by the strong increase of ϵ' towards

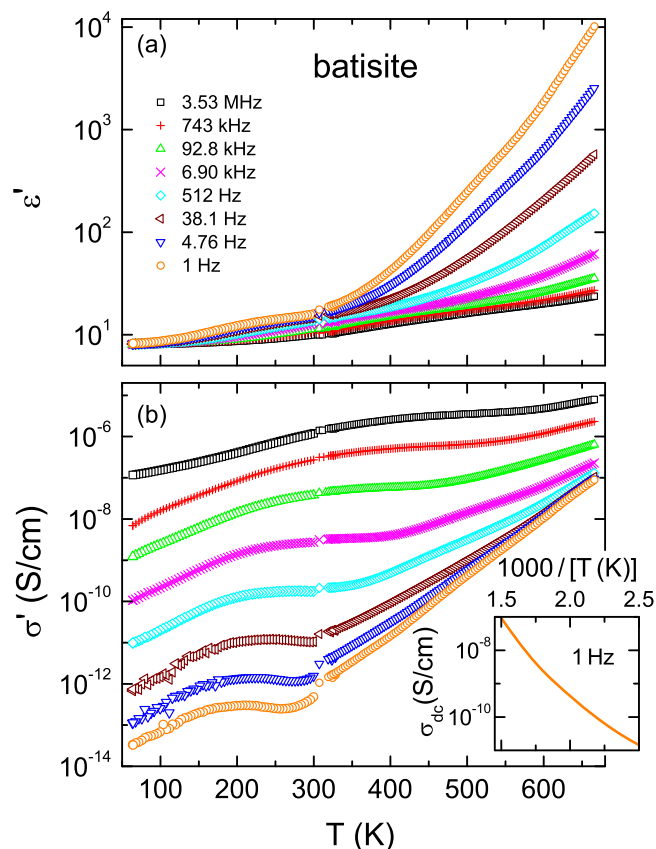


Figure 1 | Temperature dependence of the measured electrical properties of batisite. Dielectric constant (a) and conductivity (b) are shown as obtained at various frequencies (for the sake of clarity, curves are only shown for part of the investigated frequencies). The inset shows the conductivity at 1 Hz, which corresponds to the dc conductivity at $T > 400$ K, in an Arrhenius representation.

very high values, mentioned above (e.g., for the curve at 1 Hz the point of inflection of the step is located at about 180 K).

In most of the frequency and temperature ranges covered by our experiments, σ' strongly increases with frequency [Fig. 1(b)]. For the higher temperatures, where the relaxation peaks no longer contribute to σ' , this increase signifies ac conductivity arising from the hopping of localized charge carriers as will be explained in more detail in the next paragraph. However, at the lowest frequencies and high temperatures, σ' does not depend on frequency. This becomes obvious, e.g., by the agreement of the 1 and 4.76 Hz curves at $T > 500$ K in Fig. 1(b). In this region, the frequency independent σ' can be identified with the dc conductivity of batisite. Comparing the curve at 1 Hz with that at the next-lowest measured frequency of 1.7 Hz (not shown in Fig. 1), indicates that $\sigma'(T)$ at 1 Hz corresponds to the dc conductivity for temperatures above about 400 K. σ_{dc} obtained in this way is plotted in the inset of Fig. 1 in Arrhenius representation. The found absence of a linear region in $\sigma_{dc}(1/T)$ demonstrates that the dc conductivity of batisite does not follow the thermally activated behaviour expected for conventional band conduction, i.e., $\sigma_{dc} \propto \exp[-E_{\sigma}/(k_B T)]$, with an activation energy E_{σ} . This finding points to electronic hopping conductivity, where such deviations are commonly observed^{11,12}. It also indicates that the hopping transport in batisite most likely is not of ionic nature, which commonly leads to Arrhenius behaviour of the dc conductivity (see, e.g., refs. 13,14). Finally, it should be noted that the results of Fig. 1 reveal that batisite is a poor conductor. For example, at room temperature the conductivity at 1 Hz reaches values as low as 10^{-12} S/cm. This value would be too low to be detected by most conventional four-point techniques

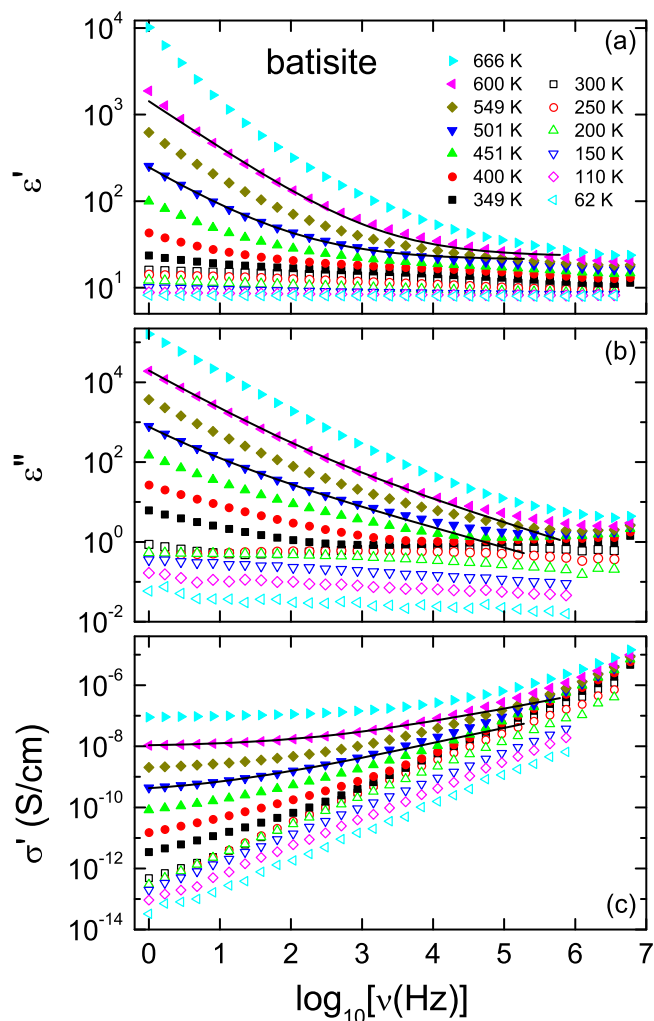


Figure 2 | Frequency dependence of the measured electrical properties of batisite. The dielectric constant (a), dielectric loss (b) and conductivity (c) are shown as obtained at various temperatures. The lines are fits of the spectra at 501 and 601 K using Eqs. (1) and (2), performed simultaneously for ϵ' and σ' [the lines in (b) were calculated from those in (c)].

and only the extremely high sensitivity of the used dielectric devices enables its detection.

Figure 2 shows the frequency dependence of the dielectric permittivity [real and imaginary part; frames (a) and (b), respectively] and the conductivity (c) of batisite measured at various temperatures. While at low temperatures (open symbols) $\epsilon'(v)$ is only weakly frequency dependent, at higher temperatures (closed symbols) it exhibits a smooth decrease with increasing frequency. Similar behaviour is found for $\epsilon''(v)$. In $\sigma'(v)$, the high-temperature spectra show a plateau at low frequencies before starting to increase with increasing frequency. At lower temperatures a continuous increase is observed throughout the whole frequency range. This overall behaviour of $\epsilon'(v)$, $\epsilon''(v)$ and $\sigma'(v)$ is typical for hopping conductivity of localized charge carriers, which leads to an approximate power-law increase of the conductivity, $\sigma' \propto v^s$ with $s < 1$ ^{11,15}. Such behaviour corresponds to the so-called “universal dielectric response” (UDR), observed in various materials¹⁶. Taking into account the dc conductivity σ_{dc} , one arrives at

$$\sigma' = \sigma_{dc} + \sigma_0 v^s \quad (1)$$

(σ_0 is a prefactor). Via the Kramers-Kronig relation, Eq. (1) leads to a corresponding power law in the imaginary part of the conductivity, namely $\sigma'' = \tan(s\pi/2)\sigma_0 v^s$ (ref. 16). As the dielectric constant is



directly related to σ'' via $\varepsilon' = \sigma''/(2\pi\nu\varepsilon_0)$ (with ε_0 the permittivity of vacuum), hopping conduction is expected to lead to

$$\varepsilon' = \tan(s\pi/2) \sigma_0/(2\pi\varepsilon_0) \nu^{s-1} + \varepsilon_\infty. \quad (2)$$

Here ε_∞ was added to account for the high-frequency limit of the dielectric constant arising from the ionic and electronic polarizability. Equation (2) implies a divergence of the dielectric constant for low frequencies, which explains the high values of ε' revealed in Figs. 1(a) and 2(a)⁸. To check if hopping conductivity indeed governs the high-temperature dielectric response of batisite, we have fitted the spectra for 501 and 600 K using Eqs. (1) and (2). The fits were simultaneously performed for $\varepsilon'(\nu)$ and $\sigma'(\nu)$. In $\varepsilon'(\nu)$ a good agreement of fit and experimental data was obtained. However, in the loss and conductivity only the results at the lower frequencies could be well described by this approach while marked deviations show up at high frequencies. They can be ascribed to the influence of the relaxation process, already mentioned in the above discussion of Fig. 1(b). The fit curves shown as lines in Fig. 2 were thus obtained by disregarding the results at the highest frequencies.

Just as for the temperature dependence, relaxation processes should lead to peaks in the frequency dependence of ε'' , too^{9,10}. Already in Fig. 2(b) such behaviour can be suspected for the lower temperatures (open symbols) and it becomes clearly obvious in the magnified view of this region provided by Fig. 3. The detected loss peaks strongly shift to lower frequencies with decreasing temperature, finally dropping out of the investigated frequency window. This mirrors the continuous slowing down of the relaxational dynamics. Via the relation $\tau \approx 1/(2\pi\nu_p)$, the relaxation time τ , characterizing the mobility of the relaxing entities, can be estimated from the peak frequencies ν_p ⁹. The inset of Fig. 3 shows the obtained temperature dependence of τ in Arrhenius representation. The found nearly linear increase of $\log[\tau(1/T)]$ corresponds to thermally acti-

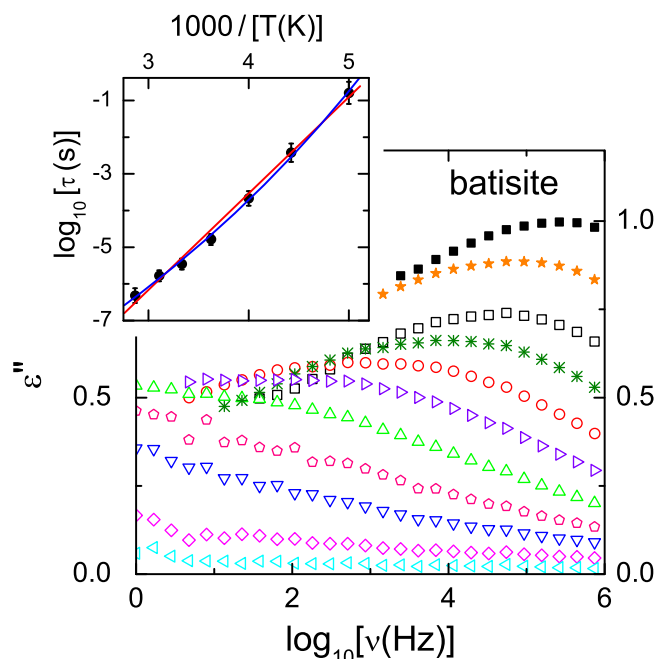


Figure 3 | Frequency dependence of the dielectric loss of batisite. The spectra were measured at various temperatures (from top to bottom: 349 K, 322 K, 300 K, 276 K, 250 K, 226 K, 200 K, 174 K, 150 K, 110 K, 62 K; to keep Fig. 1 readable, only part of these temperatures were shown there). The inset shows the temperature dependence of the relaxation times calculated from the loss-peak frequencies in an Arrhenius representation. The red line is a linear fit demonstrating thermally activated behaviour with an energy barrier of 0.52 eV. The blue line shows a fit with the VFT law ($\tau_0 = 1.1 \times 10^{-11}$ s, $B = 2100$ K, $T_{VF} = 78$ K).

vated behaviour, $\tau \propto \exp(E/k_B T)$. From the slope of the linear fit curve (red line in the inset of Fig. 3) we deduce a hindering barrier $E = 0.52$ eV. However, a close inspection of the inset of Fig. 3 reveals a small but systematic deviation of $\log[\tau(1/T)]$ from linear behaviour. The blue line is a fit with the empirical Vogel-Fulcher-Tammann (VFT) law, $\tau = \tau_0 \exp[B/(T - T_{VF})]$ ^{17–19}, which leads so somewhat better agreement with the experimental data. In analogy to the interpretation of the commonly found VFT behaviour of supercooled liquids^{10,20–22}, this finding seems to indicate an increasing cooperativity of the relaxational motions at low temperatures.

To further investigate the possible occurrence of ferroelectricity in batisite, Fig. 4 shows the results of electric-field dependent polarization measurements performed between 60 and 600 K. For ferroelectric materials, characteristic $P(E)$ hysteresis curves exhibiting a saturation of P at high absolute values of the field are expected⁷. However, Fig. 3 reveals purely elliptical hysteresis loops without any trace of saturation effects. Such behaviour is typical for lossy capacitors and can be explained without invoking any ferroelectric ordering when considering the relation $P = \varepsilon_0(\varepsilon - 1)E$. For any dielectric material, contributions to the dielectric loss (e.g., the dc conductivity) make ε a complex quantity. This causes a phase shift between P and E explaining the observed ellipses. Subtracting a horizontal ellipse from the measured hysteresis should correct for these loss contributions and reveal the in-phase component only. For the present results this procedure leads to the solid lines in Fig. 4. The grey dashed lines represent linear fit curves, demonstrating purely linear polarization in batisite.

Discussion

Batisite reveals the typical signatures of hopping conductivity of localized charge carriers leading to the characteristic ν^s power law of the frequency-dependent conductivity. In principle, such a power law can arise for both ionic and electronic hopping transport. However, for crystalline materials electronic conductivity is the more common charge-transport process and the found deviations of the dc conductivity of batisite from an Arrhenius law (inset of Fig. 1) also point to electron hopping^{11,12}. In electronic conductors, charge-carrier localization of electrons or holes is driven by disorder. It can be due to an amorphous structure or substitutional disorder caused by doping^{11,15}, both not being applicable for the present case. However, localization of charge carriers and hopping conductivity even can

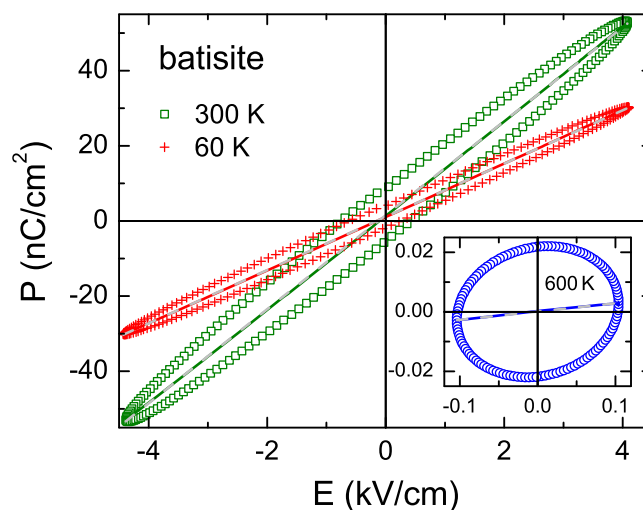


Figure 4 | Ferroelectric polarization P of batisite. P is shown as a function of external electric field E at 113 Hz and three temperatures (symbols). The coloured lines show the results corrected for loss contributions by subtracting horizontal ellipses. The grey dashed lines are linear fits demonstrating a perfectly linear behaviour of the corrected $P(E)$ curves.



occur in nominally pure, crystalline materials due to slight deviations from stoichiometry or lattice imperfections. For example, hopping conductivity was also found in numerous single-crystalline transition-metal oxides (see, e.g., refs. 8,23–26). A similar mechanism can be assumed for batisite.

In addition, we found evidence for a relaxational process at the lower temperatures, $T < 350$ K, revealing an energy barrier of the relaxing entities of about 0.5 eV. The static dielectric constant ϵ_s of this relaxation process, which can be read off from the upper plateau value of the corresponding steps in Fig. 1(a), is about 15–20. This moderate value speaks against a non-intrinsic origin of this spectral feature due to electrode polarization, which usually leads to much larger values of ϵ_s ^{8,27}. Intrinsic relaxational processes can arise from the reorientation of dipolar molecules (or molecule parts) or from the off-centre motion of a charged particle within a double (or multiple) well potential. The structure of batisite comprises distorted transition-metal oxygen octahedra (TiO_6) with the titanium ions at off-centre positions. One may speculate that motions of the titanium ions within the distorted octahedra lead to the observed relaxation, similar to the mechanism recently proposed to explain the relaxation processes in various perovskite rare-earth manganites²⁸.

We find no indications of ferroelectric order in the dielectric properties of batisite. One may ask if contributions from the detected conductivity could obscure the expected signatures of polar order in the dielectric constant. At first, as mentioned above, the conductivity of batisite is rather low. In literature there are many reports where clear signatures of ferroelectricity in dielectric data were found for materials having much higher conductivity than batisite. Examples from our group are CdCr_2S_4 ²⁹ with a room-temperature conductivity of 10^{-6} S/cm³⁰, κ -(BEDT-TTF)₂Cu[N(CN)₂]Cl with a conductivity at the ferroelectric transition of about 10^{-5} S/cm³¹, or magnetite³² with a conductivity between 10^{-3} and 10^{-11} S/cm below the Verwey transition³³. As discussed above, only the ac conductivity, i.e. the ν^s power law contributes to the dielectric constant. An inspection of Fig. 1(a) reveals that this is only the case for the lower frequencies and temperatures above about 300 K. At $T < 300$ K, only a small dielectric constant of the order of 10 and no peak is seen, both indicating the absence of ferroelectric order. At higher temperatures, ϵ' starts to assume high values at low frequencies due to hopping conductivity. However, these conductivity contributions obviously play no role at the highest frequencies, above some 100 kHz. The fact that no peak and only moderate values of ϵ' are seen here, also points to the absence of ferroelectric ordering. However, it should be noted that in a special class of ferroelectric materials, the order-disorder ferroelectrics, the signature of ferroelectricity can become suppressed at high frequencies^{7,31}. Thus we cannot completely rule out that the ac conductivity contribution in batisite has just the right amplitude, temperature and frequency dependence to hide the signature of order-disorder ferroelectricity in Fig. 1(a) but such a scenario at least seems unlikely.

The absence of ferroelectricity is corroborated by our polarization measurements, which provide no evidence for ferroelectric polarization in batisite and instead reveal the typical characteristics of a linear lossy dielectric. This is in full accord with our findings from dielectric spectroscopy. One should note that at the highest investigated temperatures, due to the non-negligible conductivity the $P(E)$ measurements were restricted to relatively moderate fields (cf. inset of Fig. 4). It is clear that we cannot fully exclude that batisite shows a ferroelectric transition at very high temperature, maybe even above the investigated temperature region, which would lead to the detection of rather small dielectric-constant values at low temperatures (far below the ferroelectric transition temperature, where a peak in $\epsilon'(T)$ is expected⁷) and which would make the detection of $P(E)$ hysteresis loops difficult.

In summary, within the investigated broad temperature and frequency space of the present work, no indications for the typical

signatures of polar order in batisite are found making it unlikely that this material is ferroelectric. As the SHG observed in batisite¹ points to a non-centrosymmetric structure, this material is piezoelectric⁶, but most likely it is not ferroelectric. Precise structural investigations of single-crystalline samples are planned to finally clarify this issue.

Methods

Polycrystalline samples of $\text{BaNa}_2\text{Ti}_2\text{Si}_4\text{O}_{14}$ (batisite) were synthesized by the standard solid-state reaction route from BaCO_3 , dried (150°C) Na_2CO_3 , TiO_2 and SiO_2 . The materials were thoroughly ground and mixed and subsequently heated to 200°C to check for any weight loss, which was not observed. Subsequently the powder was cold-pressed into pellets and reacted for 12 h at 900°C , then reground, and repelletized. The final sintering was done at 950°C in air for 24 h with 8 h periods for heating and cooling. The resulting samples are of a white, greyish colour. Powder x-ray diffraction proved the obtained material to be single phase. For the dielectric measurements, the sintered pellets were coated with silver paint contacts on opposite sides of the disk-shaped samples.

The complex permittivity $\epsilon^* = \epsilon' - i\epsilon''$ and the real part of the conductivity σ' at frequencies $1 \text{ Hz} \leq \nu \leq 6 \text{ MHz}$ were determined using a frequency-response analyser (Novocontrol alpha-Analyser)^{10,34}. The field-dependent polarization, $P(E)$, was measured using a ferroelectric analyser (TF2000, aixACCT). For sample cooling between 62 and 300 K, a closed-cycle refrigerator was employed. Measurements from room temperature up to 666 K were done in a home-made oven.

- Gopalakrishnan, J., Ramesha, K., Rangan, K. K. & Pandey, S. In search of inorganic nonlinear optical materials for second harmonic generation. *J. Solid State Chem.* **148**, 75–80 (1999).
- Bloembergen, N. & Pershan, P. S. Light waves at the boundary of nonlinear media. *Phys. Rev.* **128**, 606–622 (1962).
- Williams, D. J. Organic polymeric and non-polymeric materials with large optical nonlinearities. *Angew. Chem. Int. Ed. Engl.* **23**, 690–703 (1984).
- Nikitin, A. V. & Belov, N. V. Crystal structure of batisite $\text{Na}_2\text{BaTi}_2\text{Si}_4\text{O}_{14} = \text{Na}_2\text{BaTi}_2\text{O}_2(\text{Si}_4\text{O}_{12})$. *Dokl. Akad. Nauk SSSR, Earth Science Sections* **146**, 142–143 (1962).
- Schmahl, W. W. & Tillmanns, E. Isomorphic substitutions, straight Si-O-Si geometry, and disorder of tetrahedral tilting in batisite, $(\text{Ba},\text{K})(\text{K},\text{Na})\text{Na}(\text{Ti},\text{Fe},\text{Nb},\text{Zr})\text{Si}_4\text{O}_{14}$. *Neues Jahrb. Mineral. Monatsh.* **1987**, 107–118 (1987).
- Kravchenko, S. M., Vlasova, Ye. V. & Pinevich, N. G. Batisite, a new mineral. *Dokl. Akad. Nauk SSSR, Earth Science Sections* **146**, 805–808 (1962).
- Lines, M. E. & Glass, A. M. *Principles and applications of ferroelectrics and related materials*. (Clarendon Press, Oxford, 1979).
- Lunkenheimer, P. et al. Colossal dielectric constants in transition-metal oxides. *Eur. Phys. J. Special Topics* **180**, 61–89 (2010).
- Kremer, F. & Schönhals, A. (eds.), *Broadband Dielectric Spectroscopy*. (Springer, Berlin, 2002).
- Lunkenheimer, P., Schneider, U., Brand, R. & Loidl, A. Glassy dynamics. *Contemp. Phys.* **41**, 15–36 (2000).
- Long, A. R. Frequency-dependent loss in amorphous semiconductors. *Adv. Phys.* **31**, 553–637 (1982).
- Mott, N. F. & Davis, E. A. *Electronic Processes in Non-Crystalline Materials*. (Clarendon Press, Oxford, 1979).
- Pimenov, A., Ullrich, J., Lunkenheimer, P., Loidl, A. & Rüscher, C. H. Ionic conductivity and relaxations in $\text{ZrO}_2\text{-Y}_2\text{O}_3$ solid solutions. *Solid State Ionics* **109**, 111–118 (1998).
- Sammes, N. M., Tompsett, G. A., Näfe, H. & Aldinger, F. Bismuth Based Oxide Electrolytes - Structure and Ionic Conductivity. *J. European Ceramic Society* **19**, 1801–1826 (1999).
- Elliott, S. R. A.c. conduction in amorphous chalcogenide and pnictide semiconductors. *Adv. Phys.* **36**, 135–218 (1987).
- Jonscher, A. K. *Dielectric Relaxations in Solids*. (Chelsea Dielectrics Press, London, 1983).
- Vogel, H. Das Temperaturabhängigkeitsgesetz der Viskosität von Flüssigkeiten. *Z. Phys.* **22**, 645–646 (1921).
- Fulcher, G. S. Analysis of recent measurements of the viscosity of glasses. *J. Am. Ceram. Soc.* **8**, 339–355 (1925).
- Tammann, G. & Hesse, W. Die Abhängigkeit der Viskosität von der Temperatur bei unterkühlten Flüssigkeiten. *Z. Anorg. Allg. Chem.* **156**, 245–257 (1926).
- Ediger, M. D., Angell, C. A. & Nagel, S. R. Supercooled liquids and glasses. *J. Phys. Chem.* **100**, 13200–13212 (1996).
- Debenedetti, P. G. & Stillinger, F. H. Supercooled liquids and the glass transition. *Nature* **310**, 259–267 (2001).
- Bauer, Th., Lunkenheimer, P. & Loidl, A. Cooperativity and the freezing of molecular motion at the glass transition. *Phys. Rev. Lett.* **111**, 225702 (2013).
- Pike, G. E. Ac Conductivity of Scandium Oxide and a New Hopping Model for Conductivity. *Phys. Rev. B* **6**, 1572–1580 (1972).
- Lunkenheimer, P., Resch, M., Loidl, A. & Hidaka, Y. AC conductivity in La_2CuO_4 . *Phys. Rev. Lett.* **69**, 498–501 (1992).



25. Lunkenheimer, P. *et al.* Dielectric properties and dynamical conductivity of LaTiO_3 : From dc to optical frequencies. *Phys. Rev. B* **68**, 245108 (2003).
26. Renner, B. *et al.* Dielectric behavior of copper tantalum oxide. *J. Appl. Phys.* **96**, 4400–4404 (2004).
27. Lunkenheimer, P. *et al.* Origin of apparent colossal dielectric constants. *Phys. Rev. B* **66**, 052105 (2002).
28. Schrettle, F. *et al.* Relaxations as key to the magnetocapacitive effects in the perovskite manganites. *Phys. Rev. Lett.* **102**, 207208 (2009).
29. Hemberger, J. *et al.* Relaxor ferroelectricity and colossal magnetocapacitive coupling in ferromagnetic CdCr_2S_4 . *Nature* **434**, 364–367 (2005).
30. Lunkenheimer, P., Fichtl, R., Hemberger, J., Tsurkan, V. & Loidl, A. Relaxation dynamics and colossal magnetocapacitive effect in CdCr_2S_4 . *Phys. Rev. B* **72**, 060103(R) (2005).
31. Lunkenheimer, P. *et al.* Multiferroicity in an organic charge-transfer salt that is suggestive of electric-dipole driven magnetism. *Nature Mater.* **11**, 755–758 (2012).
32. Schrettle, F., Krohns, S., Lunkenheimer, P., Brabers, V. A. M. & Loidl, A. Relaxor ferroelectricity and the freezing of short-range polar order in magnetite. *Phys. Rev. B* **83**, 195109 (2011).
33. Kobayashi, M., Akishige, Y. & Sawaguchi, E. Dielectric and Conducting Properties of Single Crystal of Magnetite below the Verwey Point. *J. Phys. Soc. Jpn.* **55**, 4004–4052 (1986).
34. Schneider, U., Lunkenheimer, P., Pimenov, A., Brand, R. & Loidl, A. Wide range dielectric spectroscopy on glass-forming materials: An experimental overview. *Ferroelectrics* **249**, 89–98 (2001).

Acknowledgments

This work was supported by the Deutsche Forschungsgemeinschaft via the Transregional Collaborative Research Center TRR 80 and by the BMBF via ENREKON.

Author contributions

W.W.S. initiated the research and provided the samples for the experiments. F.G. prepared the sample material. A.L. and P.L. supervised the project. S.K. and P.L. performed the dielectric measurements and analysed the data. P.L. wrote the paper with contributions from W.W.S. All authors discussed the results and commented on the manuscript.

Additional information

Competing financial interests: The authors declare no competing financial interests.

How to cite this article: Lunkenheimer, P., Krohns, S., Gemander, F., Schmahl, W.W. & Loidl, A. Dielectric Characterization of a Nonlinear Optical Material. *Sci. Rep.* **4**, 6020; DOI:10.1038/srep06020 (2014).



This work is licensed under a Creative Commons Attribution-NonCommercial-NoDerivs 4.0 International License. The images or other third party material in this article are included in the article's Creative Commons license, unless indicated otherwise in the credit line; if the material is not included under the Creative Commons license, users will need to obtain permission from the license holder in order to reproduce the material. To view a copy of this license, visit <http://creativecommons.org/licenses/by-nc-nd/4.0/>